Optica Applicata, Vol. XXVI, No. 3, 1996

Semiconductor corrugated surface structures produced using interference method

T. TKACZYK

Faculty of Precision Mechanics, Warsaw University of Technology, ul. Chodkiewicza 8, 02–525 Warszawa, Poland.

B. MROZIEWICZ

Institute of Electron Technology, al. Lotników 32/46, 02–668 Warszawa, Poland.

A short analysis of patterns produced on a flat surface by means of the interference method is given. Two optical systems: Lloyd's and Twyman–Green's, used in this work to obtain high and low line frequency patterns, respectively, are described. Photolithographic and etching processes that lead to corrugated surface are discussed and results obtained with three different etchants are compared. Methods of testing of the corrugated surfaces are presented and the results are compared with those predicted by the theory.

1. Introduction

Semiconductor structures with corrugated surface find application in many photonic devices, just to mention an abundance of DFB (Distributed Feedback) and DBR (Distributed Bragg Reflectors) lasers [1], [2]. Recently, they have been used to provide optical coupling in the monolithically integrated photonic devices like MOPAs (Master Oscillator Power Amplifier) [3].

In this paper, we describe some experimental work that was mainly aimed at development of procedure that would allow us to produce stripe patterns on the mirrors of Fabry–Perot semiconductor lasers to modify their output beam [4]. Dimensions of the stripes in this application are in the range of 5–7 μm or 200–143 lines/mm. However, since corrugated structures with a much higher line frequency find immense use in photonic devices, investigations were extended to fabricate corrugations with line spacing corresponding to as many as 1200 lines/mm. Light interference method was applied here as the most straightforward although some other approaches have recently been presented in relation with gratings produced on optical fibres [5]–[7].

2. Principles of writing diffraction gratings on semiconductor by means of the interference method

Semiconductor wafers with flat and smooth surfaces only are adequate for this

process which essentially consists of four stages:
- coating with photoresist,
- exposing to light fringe pattern,
- developing the pattern inscribed in the photoresist,
- etching of the pattern in areas uncovered by the photoresist to produce corrugations.

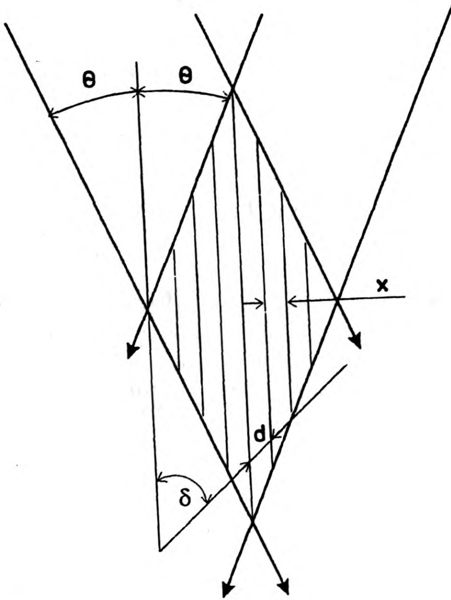

Fig. 1. Interference fringe pattern employed for writing diffraction gratings

The light fringe pattern used in the exposition process is formed by interference of two mutually coherent beams. If the angle between these beams is equal to 2θ, as shown in Fig. 1, the period of the fringe pattern x will be equal to

$$x = \frac{\lambda}{2\sin\theta}.$$

If the semiconductor wafer is inserted into the interference field at an angle δ (Fig. 1), then the inscribed fringe pattern will have the period d

$$d = \frac{\lambda}{2\sin\theta\sin\delta}.$$

Thus, the smallest theoretically feasible period equals $\lambda/2$ and can be obtained for $\delta = 0°$ and $\theta = 90°$. In practice, the "grazing" waves ($\theta = 90°$) cannot be used and the lowest but still precise period can be obtained for θ equal to about 60°. The period d will then be equal to 0.6λ, which means that for the wavelength $\lambda = 442$ nm (He-Cd laser) it is equal to 256 nm (3800 lines/mm). It is obvious that in manufacturing

the structures with higher values of the period the physical restrictions described above are not encountered and limitations depend only on the particular configuration of the writing set-up [8], [9].

2.1. Conditions of writing

One of the most important requisites in the fabrication process of periodic structures is to keep the interference fringe pattern stationary during the exposure. Any movement will result in reduction of the effective local exposure and thus of the groove depth. There are many factors that can cause movement of the interference fringes during the exposure process. The most important include mechanical disturbances from the surroundings, thermal drift of the optical components and of the interfering beams, air fluctuations and shifts of the laser output mode [10]. We used a holographic table (Spindler–Hoyer) which isolated our set-up from the environment. Moreover, the whole optical set-up was covered by a plastic tent to protect it against the air fluctuations. All experiments were carried out one hour after the laser was switched on to assure stability of its work.

Plane wave fronts are required to obtain correct shape of the lines in diffraction gratings. This problem can be solved in two ways: one is to use spherical waves with adequate radius which allows us to neglect the spherical shape of the wave front [11], and the second is based on using a highly collimating optics. The main disadvantages of the first method are large dimensions of the optical system (about 2 m radius for 20×20 mm^2 field) and significant light losses. That was the reason why we used a collimator objective (400 mm focus) adjusted with a shearing plate. The estimated quality of the wave front behind the collimator, as expressed in deviation from the plane wave front, was smaller than $\lambda/5$ on a diameter of 80 mm. Considering that the mirrors and beam splitters used have been corrected to $\lambda/20$ (for 120×90 mm dimensions) and that the working field was 20×20 mm, the achieved deviation is small enough to be acceptable.

3. Optical system

Two optical systems: Lloyd interferometer and Twyman–Green interferometer were tested for writing the 1200 lines/mm and 75–150 lines/mm gratings, respectively. Hovewer, only the second set-up is described here in detail due to its importance to the applications considered. The description of high frequency gratings technology is given in [12].

The Twyman–Green interferometer was used for producing periodic structures with line frequency lower than 300 lines/mm. It consisted of the He-Cd laser (120 mW CW, TEM_{00} mode, wavelength 442 nm), and the components displayed in Fig. 2. The plane wave front after passing the collimator is divided by a beam splitter B and irradiates mirrors M_1 and M_2. Reflected beams cross the beam splitter and interfere in the space, respectively. When the mirrors are perpendicular to each other an infinite fringe pattern is obtained. If one of the mirrors is tilted at the angle β, we observe phenomena similar to those of the optical wedge in Fizeau [13] inter-

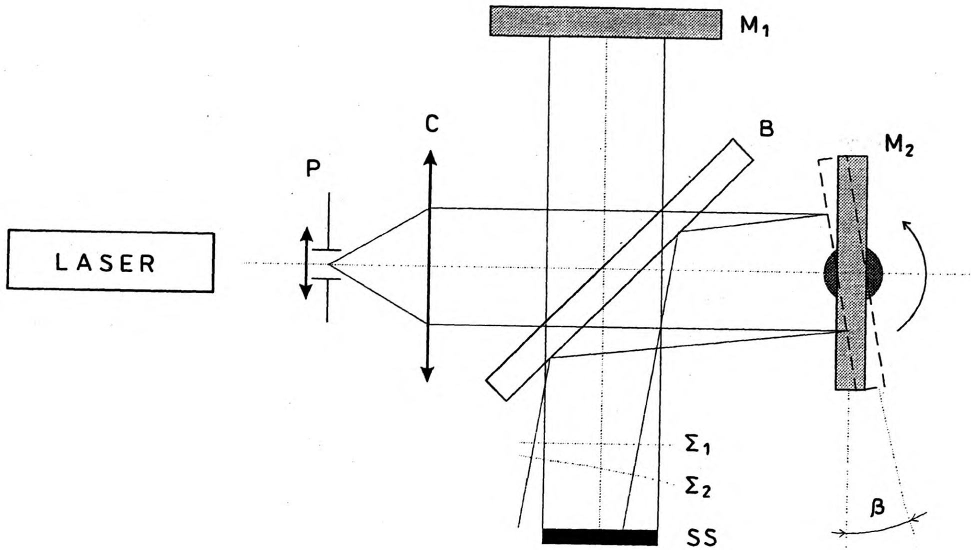

Fig. 2. Twyman—Green interferometer for writing low line frequency (up to 300 lines/mm) gratings. The set-up consists of a He-Cd laser, P — pinhole set-up, C — collimator objective, SS — semiconductor substrate, beam splitter B and two mirrors M_1, M_2

ferometer (wave front Σ_1 interferes with wave front Σ_2) and a finite fringe pattern distribution is produced. The equation for the optical wedge is simple: $\beta = \lambda K/2nL$, where K is the number of fringes for the whole length L (in millimetres), n is the refractive index, and λ is the light wavelength. It thus determines the line frequency f of the exposed structure, which in the case of $L = 1$ mm is equal to $f = 2n\beta/\lambda$.

Therefore, dimensions of interference field depend on the wavelength λ and the tilting angle β. These two parameters are fixed for a chosen line frequency and we can optimise dimensions of the written structures by changing the distance between the mirrors and the substrate (for the best contrast it should be obviously the same for both beam branches). In our experiment, we have reached effectively a 25×25 mm^2 field which was the result of a compromise between the mirror-substrate distance and the effect of the existing secondary beam-splitter reflections on the interference pattern. The angle β was adjusted in this experiment by a 5′ scale rotary table providing an accuracy of ± 5 lines/mm. However, the more precise moiré method could also be applied here if proper reference structures were available.

4. Exposure and the chemistry

4.1. Coating with a photoresist layer

This step was identical to standard procedure employed in semiconductor technology and consisted in:

- treatment of the substrates in chemical baths,
- spin-coating with photoresist,

– baking at elevated temperature (about 100 °C).

Three thicknesses of the photoresist AZ 1350 were tested: 100, 1000 and 2000 nm.

4.2. Exposing process

Discussion in this paragraph is confined to 75–150 lines/mm structures only, since procedures leading to gratings of 1200 lines/mm line density have already been described elsewhere [12], [14]. Exposure times were in the range of 20–240 s, while the development times equalled 30–90 s. Exact figures strictly relate to the particular experimental conditions and have to be adjusted accordingly. Semiconductor substrates coated with a thin layer of photoresist have to be precisely placed in the interference field. Energy of the beams should be evenly distributed over the whole exposed field, otherwise a good contrast in the grating structure will not be achieved. It also appeared that for the thicker (1 and 2 μm) photoresist layers it was difficult to obtain uniform distribution which eliminated etching possibility of these substrates. A thin (about 100 nm) photoresist layer allowed us to achieve a good structure but the photoresist stripes were narrower in comparison with the unveiled stripes of the semiconductor surface, which later caused some troubles with the etching.

4.3. Etching

Experiments were focused on etching of GaAs substrates in accordance with the main purpose of this work. All tests were carried out for the 75 lines/mm structures exposed in the AZ 1350 photoresist having thickness of 85–100 nm. Wet etching technology was applied. Different etching solutions and etching times have been tried. The purpose was to achieve as deep profile as possible before self-removing of the photoresist. In addition, some silicon periodic structures were fabricated. RIE (reactive ion etching) technology was used in that case. However, it was possible to produce only very shallow grooves because the photoresist was damaged by the

Table 1. Comparison of the etching results for different chemical compounds

Substrate	Etchant	Etching time	Groove depth	Remarks
GaAs	$H_3PO_4+H_2O_2+$ethylene glycol (1+1+10)	9 min	345 nm	scattering surface
GaAs	$NH_4OH+H_2O_2+H_2O$ (20+7+973)	1	280	mat surface
GaAs	$HN_4OH+H_2O_2+H_2O$ (20+7+973)	3	530	mat surface
GaAs	Citroen acid$+H_2O_2$ (3+1)	2	333	mat surface
GaAs	Citroen acid$+H_2O_2$ (3+1)	4	585	mat surface
Silicon	$CF_4+4\%O_2$ (RIE process)	5	320	scattering surface

active chemicals used in the process. Results of the etching experiments are summarised in Table 1. Mat and scattering appearance of the grating surfaces was easy to recognise in Fourier spectrum of the structures. Mat specimens had higher share of stray light (so-called ghost effects [8]) in the intensity distribution of the particular diffraction orders.

5. Evaluation methods and experimental results

The usefulness of the gratings produced is measured through its quality parameters including:

– resolving power (line frequency, grating dimensions),

– quality of the diffracted wave front (straightness of lines, flatness of the surface, spectral purity),

– groove profile,

– diffraction efficiency.

A short analysis of these grating quality parameters is given below.

5.1. Quality of the diffracted wave front

The quality of the diffracted wave front gives global information about the straightness of the lines and flatness of the substrate. Shape of the wave front behind the diffraction grating is a combined result of these two factors:

$$E_{+1} \simeq \exp\{i[(2\pi/d)u(x,y)+(2\pi/\lambda)w(x,y)]\}$$

where d is the spatial period of grating , $u(x,y)$ is the function corresponding to the departure of the grating lines from straightness [14], $w(x,y)$ is the shape of the substrate [14], and λ is the wavelength of the illuminating beam.

Straightness of the lines in a corrugated structure depends on the quality of the optical elements used in the writing system (*e.g.*, aberrations of elements), influence of surroundings, chemical process, *etc.*, (one possibility of estimating the grating quality is to apply the Rayleigh resolution criterion [8], however it is based on quite strong conditions and gives only a qualitative, initial evaluation). Fabricated structures were examined in the Lloyd interferometer arrangement (Fig. 3) using grating interferometry method (that is, based on the interference between $+1$ and -1 orders of the tested gratings). In this method, two plane wave fronts illuminate the diffraction periodic structure under ± 1st order angle, respectively. Then the $+1$ diffracted order interferes with -1 diffracted order giving in result information about the shape of the lines in the form of an interferogram [6]

$$I(x,y) \simeq 2\{1+\cos(4\pi/d)u(x,y)\}.$$

Fringe pattern was registered on a CCD camera and analysed by an automatic fringe pattern analysis system (Fig. 3), which is based on a spatial-carrier phase shifting technique (SCPS) [14]. As a result, the maps $u(x,y)$ for investigated gratings are obtained. The cross-sections A–A are presented in Fig. 4, and show dif-

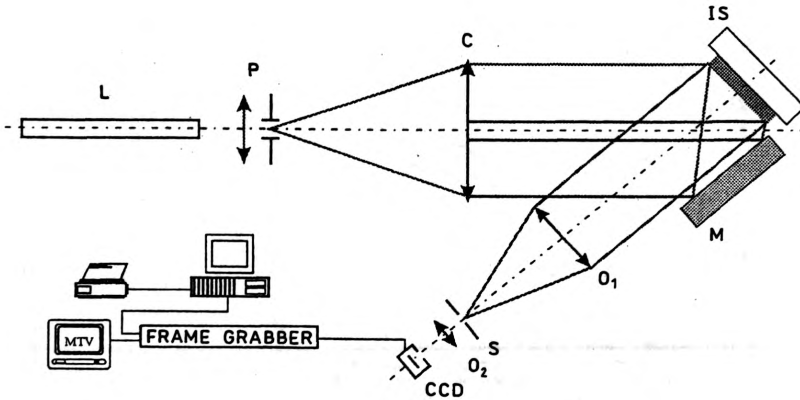

Fig. 3. Lloyd interferometer connected with an automatic fringe pattern analysis system. L — laser He-Ne, P — pinhole set-up, C — collimator objective, IS — investigated structure, M — mirror, O1, O2 and S — set-up imaging fringe pattern on a CCD camera

ference between maximum and minimum values which are an absolute range of linearity deviation of periodic structure lines for the measured field. The results present line deviation from straightness for 1200 lines/mm grating, within the 6×4 mm field, that is, less than $\lambda/5$, and for 75 lines/mm grating, in the field 3×4 mm, it reaches about 2λ (investigations were carried out with a He-Ne laser, $\lambda = 632.8$ nm). A measurement area for 75 lines/mm structures was smaller than in the case of 1200 lines/mm frequency because of difficulties in arranging the optical system for a small diffraction angle. On both cross-section graphs, for 1200 lines/mm as well as for 75 lines/mm, it is possible to notice similar tendency of deviation from linearity. Its character suggests spherical aberration of the registration system in the written structure or defocusing of the collimator objective. Moreover, we can meet here with some slight errors in the measuring system. Anyway, the numbers we

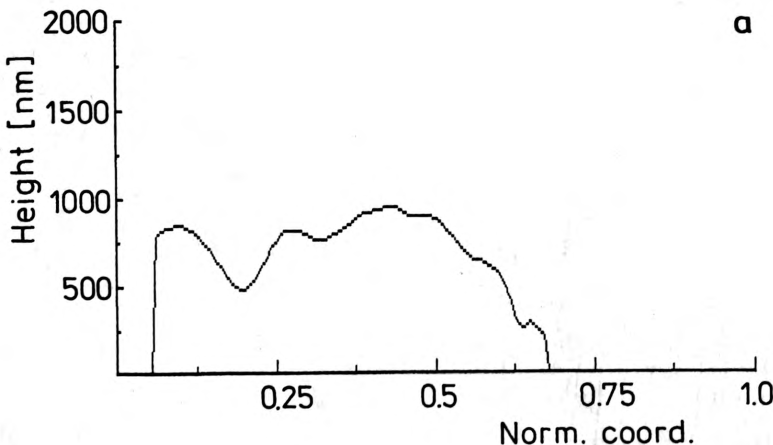

Fig. 4a

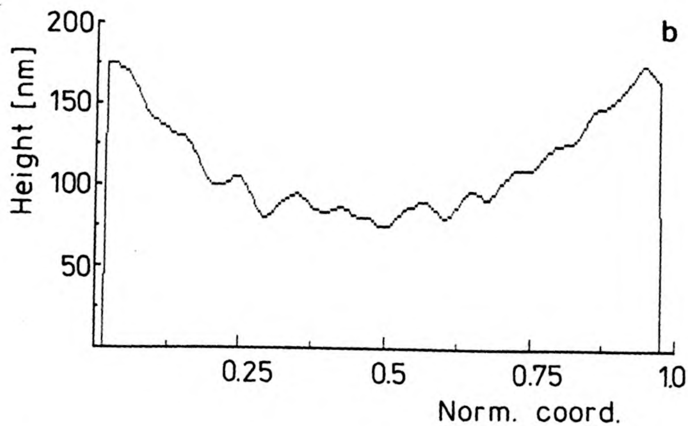

Fig. 4. Distributions of deviation of the grooves from straight lines: **a** — cross-section for 75 lines/mm grating, **b** — cross-section for 1200 lines/mm grating

observe from plots show that manufactured gratings have deviation from straightness lower than $d/10$ (where d is the grating period). Some examples of the lines shape for 75 lines/mm gratings fabricated in this work are shown in Fig. 5.

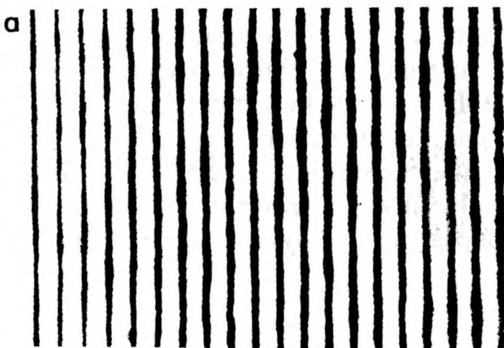

Fig. 5a

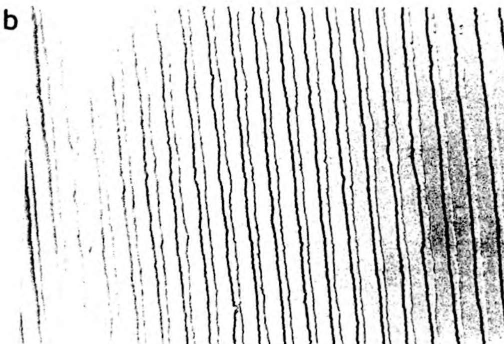

Fig 5b

c

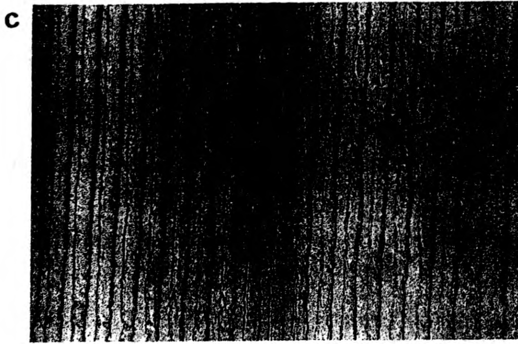

Fig. 5. Shape of the grooves for 75 lines/mm gratings: a — in photoresist, b — etched in silicon, c — etched in GaAs

Flatness of the surface of the GaAs substrates which we used during experiments is also very important for the quality of the formed wave front and should be examined with respect to the substrate dimensions. Measurements can be performed, *e.g.*, in a Fizeau interferometer arrangement applying interference between the wave fronts reflected from the reference and the tested surfaces [1], [13]. Difference between the two consecutive fringes is equal here to $\lambda/2$ and their shape allows us to estimate flatness of the examined surface. Figure 6 shows an interferogram registered on a CCD camera which proves quite high, equal to 2.5λ, deviation from the surface

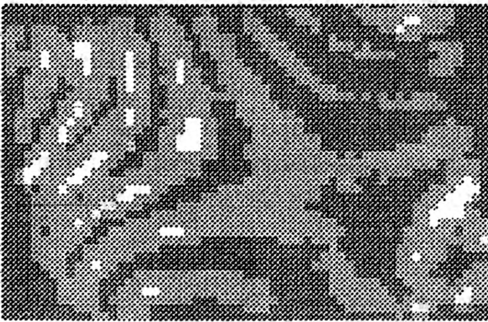

Fig. 6. Interference fringe pattern on the surface of GaAs 20×20 mm^2 substrate in a Fizeau interferometer

flatness (such value arises from small thickness of the semiconductor substrates — for good quality gratings thicker substrates should be selected).

5.2. Measurements of the line frequency

The 75 lines/mm and 150 lines/mm structures were checked using three measuring methods, including a Littrow configuration [8], an optical microscope with a measurement head and by measuring the tangent of the diffraction order angle. Theoretical periods for the examined structures were equal to $d = 13.3(3)$ μm and $d = 6.6(6)$ μm for 75 lines/mm and 150 lines/mm, respectively. The rotary positioning table could fix the angle of the mirror M_1 (in Fig. 2) with low accuracy of $\pm 2.5'$

giving possibility to reach only ±0.46 μm tolerance range of the grating period. Values of the period in the 75 and 150 lines/mm fabricated gratings, measured with the three methods mentioned above, are presented in Table 2.

Table 2. Comparison of the measured periods *d* for the 75 lines/mm and 150 lines/mm gratings while using three different measurement methods

	Littrow goniometer [μm]	Optical microscope [μm]	Geometrical dimensions [μm]
75 lines/mm (1)	13.803	13.79	13.91
(2)	13.584	13.58	13.57
150 lines/mm		6.59	
Error	±0.02	±0.2	±0.3

5.3. Efficiency distribution with regard to groove profiles

Efficiency distribution of a diffraction structure is strongly related to the profile of the grooves. Exact knowledge of the profile can therefore give efficiency distribution in a grating and vice versa.

Efficiency of a periodic structure can be defined in a couple of ways: relative efficiency is a ratio between light energy in the examined order and the whole energy of the light behind the diffraction structure, absolute efficiency is a ratio between energy in the chosen order and the entire incidence beam energy. Moreover, to gather complete information about a grating, there are always needed measurements taken for the entire light spectrum. In this work, we concentrated on the ditributions of the absolute efficiency with regard to the groove shape and therefore investigations for the whole spectrum were not necessary. Measurements of the intensity of the consecutive orders were then made with reference to the incident light beam power for only one He-Ne laser wavelength.

Table 3. Efficiency distribution between various diffraction orders for the 75 lines/mm GaAs periodic structures. The etching solutions were composed of chemicals as specified below

	Diffraction order number									
Etchant	−4	−3	−2	−1	0 [%]	1	2	3	4	Groove depth
(1)		0.32	0.37	2.85	2.14	2.85	0.37	0.30		530 nm
(2)	0.40	0.38	2.42	0.17	14.61	0.15	2.50	0.38	0.43	345 nm
(3)		0.06	0.25	5.35	0.37	5.53	0.26	0.19		585 nm

Etchants: 1 – $NH_4OH+H_2O_2+H_2O$ (20+6+973),
2 – $H_3PO_4+H_2O_2$+ethylene glycol (1+1+10),
3 – citroen acid+H_2O_2 (3+1).

In Table 3, the distributions of the absolute efficiency (in per cent) for some of the investigated 75 lines/mm GaAs structures are given (these distributions correspond to the Fourier spectra of these gratings — see next).

It follows from Table 3 that the efficiency distribution is symmetrical with respect to zero order, which proves the symmetrical profile of the grooves. Measurements of the grooves profile were performed using an α-step instrument (Tencor Instruments). The surface was sampled with a probe ended with a ball of 5 μm radius. In addition, the obtained plots were checked qualitatively by an optical sensor in which a laser beam was focused on the substrate surface and moved by a stepping motor in direction perpendicular to the lines of the grating. Different groove profiles of 75 lines/mm gratings produced on GaAs and on silicon are presented in Figs. 7 and 8, respectively. The efficiency distribution is truly related to the profile of the grating. To compare and prove experimental results furnished by both types of

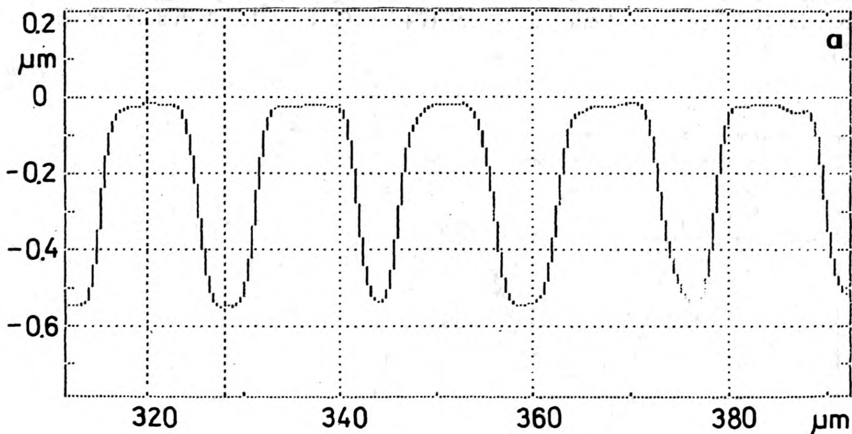

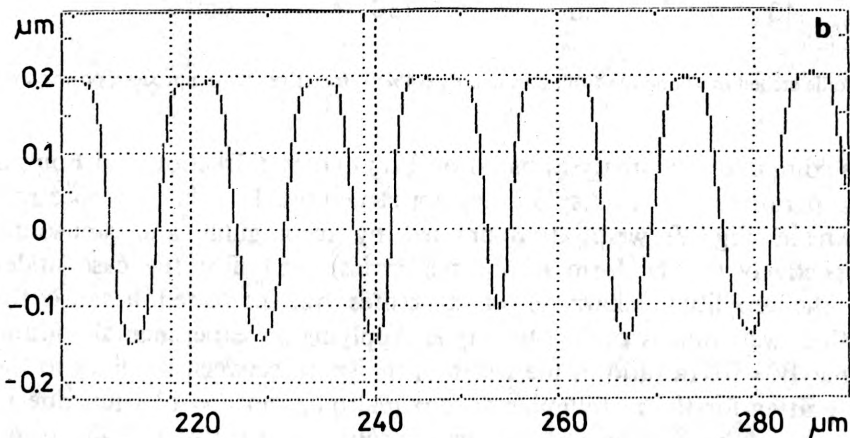

Fig. 7a,b

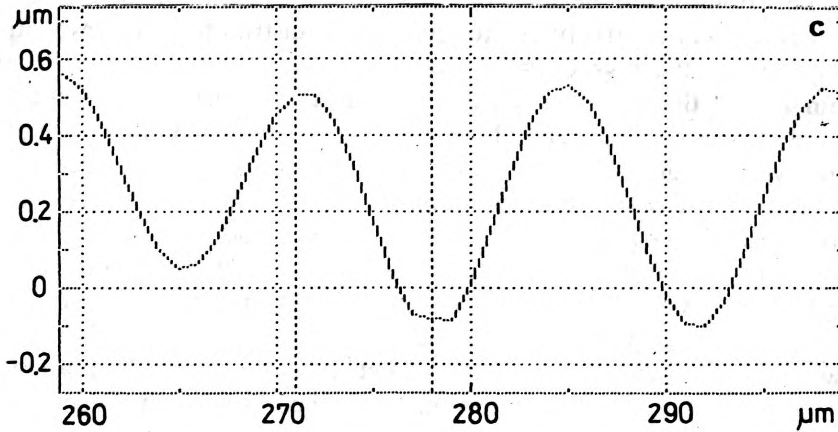

Fig. 7. Groove profiles etched in GaAs: a — for 3 minutes in $NH_4OH+H_2O_2+H_2O$ (20+6+973), b — for 9 minutes in $H_3PO_4+H_2O_2$+ethylene glycol (1+1+10), c — for 4 minutes in citroen acid$+H_2O_2$ (3+1)

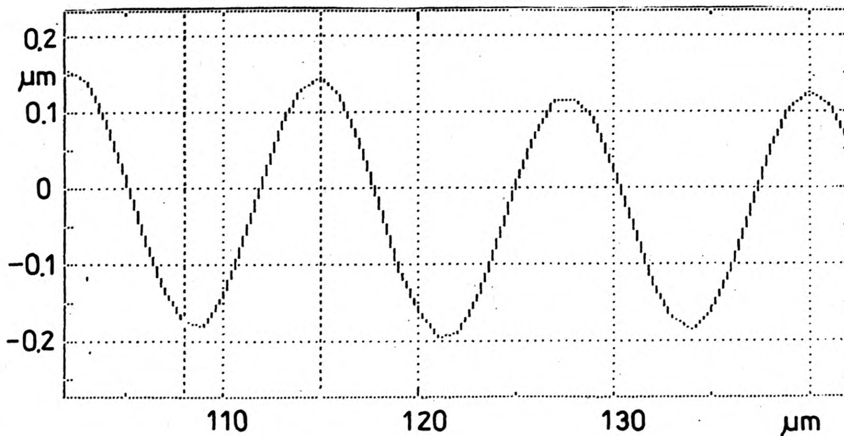

Fig. 8. Groove profile etched in silicon for 4 minutes in $CF_4+4\%O_2$ (reactive etching process, power level of 200 W)

measurements computational analyses based on Fraunhofer diffraction and Fourier spectrum were performed for GaAs 75 lines/mm structures. For that purpose real profiles (shown in Fig. 7) were approximated by rectangular and sinusoidal functions, respectively (in the form of Fourier series) [15]. For the case under consideration the amplitude character of structures was neglected because the examined gratings were mostly of the phase type. Applying the experimentally found opening number $W = 0.6$ (a ratio of the width of the space between the lines to the period of the grating for the rectangular approximation), and $d = 13.3$ µm due to reflecting character of the specimens, the Fourier spectrum was calculated. The result

of the Fourier transform of the $V_0(x) \times T(x)$, where $V_0(x)$ is the field distribution of the incident wave and $T(x)$ is the transmittance function of structure (by analogy to the approximated phase structures), is the field distrubution $V(x)$. Detected light intensity can then be expressed by multiplication of this field distribution by its conjugated function $V^*(x)$

$$I(x) = V(x) \times V^*(x).$$

Computed intensities of the Fourier spectrum for assumed approximated profiles are shown in Fig. 9.

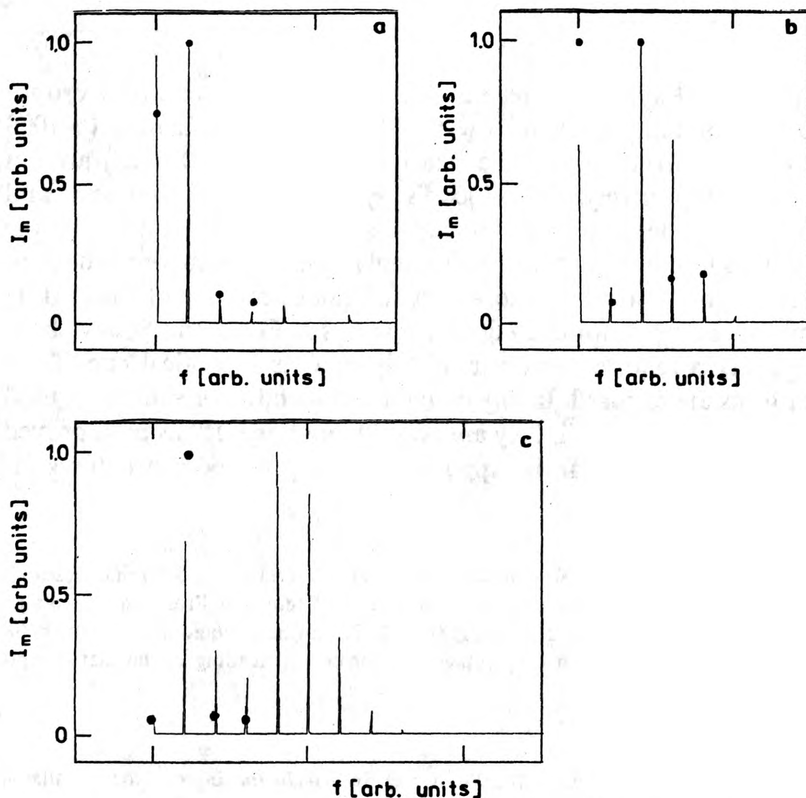

Fig. 9. Computed normalised intensity distribution I of Fourier spectrum for samples shown in Fig. 7a, b and c, respectively. Graphs are plotted for only one side of the Fourier spectrum and 0 corresponds to the zero diffraction order. Full circles marked on the plots show real values for the manufactured gratings (I_m – normalised intensity, f – spatial frequency in arbitrary units)

Graphs in Figure 9 correspond reasonably well with the measured values listed in Table 3, which have been marked on the calculated curves by full circles. Observed deviations result from the inaccurate approximation of the groove profile by the mathematical function, by the errors made while measuring this profile with a probe, and by the edge defects of the grating lines as displayed in Fig. 5. In addition, it

should be noticed that in the graph of Fig. 9c, the experimental values were normalised with respect to the 1-st order as only the first three intensity orders were measured because of the fast diminishing of the signal, while the calculations were carried out till the 6-th order and normalised to the 4-th order. It is clear from these examples that we can expect large differences in the Fourier spectrum distribution even for very subtle changes in the groove depth (more precise analysis for sinusoidal phase gratings can be found in [16]). In conclusion, phase gratings for a chosen wavelength that have to meet special Fourier distribution requirements must be fabricated under a very precisely controlled technological process.

6. Summary

Two optical arrangements: Twyman – Green and Lloyd interferometers were proposed and proved useful for fabrication of low (<300 lines/mm) and high (>1000 lines/mm) density periodic structures over a relatively large (20×20 mm^2) area of semiconductor wafers, respectively. The Lloyd's system is more compact and therefore turned out to be less sensitive to any disturbances brought in by the environment. It was also found that more precise angle positioning methods have to be used for lower line density structures to attain sufficient accuracy of the grating line density. Chemical procedures for etching corrugations in GaAs and Si have been developed but this process requires very careful adjustments to optical conditions under which the patterns are exposed. In any case the semiconductor substrates used in the process must be flat within $\lambda/2$, if they are 20×20 mm large. It has been proved that standard evaluation methods can be applied for testing periodic structures for the whole line frequency range.

Acknowledgements – This work was jointly supported by the State Committee of Scientific Research (KBN) under grant No. 8 S501 03704 and by the Authorities of the Faculty of Precision Mechanics, Warsaw University of Technology under grant No. 503/113/088/1. The authors would also like to thank Dr. A. Maląg for helpful discussions and Prof. M. Kujawińska for critical reading of the manuscript.

References

[1] MROZIEWICZ B., BUGAJSKI M., NAKWASKI W., *Physics of Semiconductor Lasers*, North-Holland, Amsterdam, Oxford, New York, Tokyo 1991.
[2] IKEGAMI T., SUDO S., SAKAI Y., *Frequency Stabilization of Semiconductor Laser Diodes*, Artech House Publishers, Boston, London 1994.
[3] OSINSKI J. S., MEHUYS D., WELCH D. F., DZURKO K. M., LANG R. J., IEEE Photon. Tech. Lett. **6** (1994), 1185.
[4] MROZIEWICZ B., Electron. Lett. **32** (1996), 329.
[5] DYER P. E., FARLEY R. J., GIEDL R., RAGDALE C., REID D., Appl. Phys. Lett. **64** (1994), 3389.
[6] ANDERSON D. Z., MIZRAHI V., ERDOGAN T., WHITE A. E., Electron. Lett. **29** (1993), 566.
[7] MALO B. HILL K. O., BILODEAU F., JOHNSON D. C., ALBERT J., Electron. Lett. **29** (1993), 1668.
[8] HUTLEY M. C., *Diffraction Gratings*, Academic Press, London 1990.
[9] LOWEN E. G., BARTLE L., Proc. SPIE **240** (1980), 27.
[10] NILSSON L. E., AHËN H., Proc. SPIE **240** (1980), 22.
[11] KOZAK S., Opt. Appl. **19** (1989), 275.

[12] MALAG A., Opt. Commun. **32** (1980), 54.
[13] JÓŹWICKI R., *Instrumental Optics* (in Polish), [Ed.] WNT, Warszawa 1970.
[14] PATORSKI K., *Handbook of the Moiré Fringe Technique*, Elsevier Sci. Publ., Amsterdam 1993.
[15] PAPOULIS S., *Systems and Transforms with Application in Optics*, McGraw-Hill Book Corp., London 1971.
[16] CATHEY W. T., *Optical Information Processing and Holography*, Wiley, New York 1974.

Received June 6, 1996
in revised form October 10, 1996